

Facile “Green” Synthesis, Characterization, and Catalytic Function of β -D-Glucose-Stabilized Au Nanocrystals

Juncheng Liu,^{*,[a, b]} Gaowu Qin,^[a] Poovathinthodiyil Raveendran,^[a] and Yukata Ikushima^{*,[a]}

Abstract: We present a straightforward, economically viable, and “green” approach for the synthesis and stabilization of relatively monodisperse Au nanocrystals with an average diameter of 8.2 nm (standard deviation, SD = 2.3 nm) by using nontoxic and renewable biochemical of β -D-glucose and by simply adjusting the pH environment in aqueous medium. The β -D-glucose acts both as reducing agent and cap-

ping agent for the synthesis and stabilization of Au nanocrystals in the system. The UV/Vis spectroscopy, Fourier transform infrared (FT-IR) spectroscopy, transmission electron microscopy (TEM), electron diffraction (ED), and X-ray diffraction (XRD)

techniques were employed to systematically characterize Au nanocrystals synthesized. Additionally, it is shown that these β -D-glucose-stabilized Au nanocrystals function as effective catalyst for the reduction of 4-nitrophenol in the presence of NaBH₄ (otherwise unfeasible if only the strong reducing agent NaBH₄ is employed), which was reflected by the UV/Vis spectra of the catalytic reaction kinetics.

Keywords: acidity • basicity • glucose • nanostructures • reduction

Introduction

Over the past decade, straightforward, economically viable, and “green” synthesis of nanoparticles has been paid wide attention in the emerging areas of nanoscience and technology.^[1] Utilization of cheap and nontoxic chemicals, environmentally benign solvents, and renewable materials are some of pivotal issues in the nanomaterials science field considering “green” synthetic strategy and industrial scale manufacture. It is well known that the reaction medium, reducing agent (RA), and capping agent (CA) are three key factors for the synthesis and stabilization of the metal nanoparticles; these factors should be considered comprehensively from an economic and “green” chemistry perspective. Most of the synthetic procedures reported to date rely heavily on organic solvents (mainly due to the hydrophobicity of the

CA used), thus inevitably resulting in a serious environmental issue while addressing industrial production. So far, some CAs such as thiols and oleic acid have been overwhelmingly utilized to prepare metal and magnetic nanoparticles in organic solvents.^[2] Nonetheless, either relatively high cost and toxicity or strict reaction conditions make these CAs less promising in industrial applications. Besides, the strong chemical bonding interaction between the particle surface and capping group not only makes it difficult to separate these CAs from the final products, but also depresses their catalytic activity (if the nanoparticles were employed as catalyst) due to the high surface coverage of the CAs on nanoparticles. Furthermore, the expensive organometallic compounds are employed as the reaction precursor in these systems, as long as a phase-transfer reagent is not utilized.^[2a,3] The use of a reverse micelle as the CA is also an effective approach to grow metal and semiconductor nanoparticles in organic solvents.^[4] The interaction between the head group of surfactant and the surface of nanoparticles is a nonchemical bond, which would consequentially influence the stability of nanoparticles in consideration of the collisions and dynamic exchange of the adjacent micelles. Although the alternative solvents such as environmentally benign supercritical CO₂ (scCO₂) and ionic liquids have been successfully utilized to synthesize nanoparticles,^[5] generally, synthetic and toxic fluorosurfactants are required for the formation of water-in-CO₂ reverse micelles (the template of nanoparticle

[a] Dr. J. Liu, Dr. G. Qin, Dr. P. Raveendran, Prof. Y. Ikushima
Tohoku Center
National Institute of Advanced Industrial Science and Technology
4-2-1 Nigatake, Miyagino-ku, Sendai 983-8551 (Japan)
Fax: (+81)022-232-7002
E-mail: liu.sam@eng.auburn.edu
y-ikushima@aist.go.jp

[b] Dr. J. Liu
Department of Chemical Engineering, Auburn University
Auburn, Alabama 36849 (USA)
Fax: (+1)334-844-2063

growth in scCO_2).^[5a] There are also problems regarding the high cost of the ionic liquid specially designed for the stabilization of nanoparticles.^[5c] There have been approaches reported^[1g,6] for the synthesis of H_2O -soluble metal nanoparticles; however, to date a unified “green” chemistry approach to the overall process of nanoparticle production, especially at ambient temperature and within a short reaction time, has seldom been reported, despite much effort having been exerted. Raveendran et al.^[1g] reported a completely “green” synthesis of silver nanoparticles using starch (CA) and β -D-glucose (RA) under heating (40°C) and long reaction time (20 h) in aqueous solution; the exact reaction and capping mechanism was not systematically investigated in the communication. Also, the synthesis of single-crystalline metal nanowires utilizing biochemicals under high temperature ($>150^\circ\text{C}$) and long reaction time (>15 h) has been successfully developed recently.^[7] More recently, our group reported an interesting self-assembly of β -D-glucose-stabilized Pt nanocrystals (by employing strong reducing agent of NaBH_4) into nanowire-like structures in basic aqueous solution.^[8]

The other concern in the “green” preparation of metal nanoparticles is the choice of RA. The majority of cases so far reported utilize RAs such as hydrazine, sodium borohydride (NaBH_4), and dimethyl formamide (DMF). All of these are highly reactive chemicals and pose potential environmental and biological risks. Although H_2 was also commonly used as RA for the metal nanoparticles synthesis, the difficulty in controlling the amount of H_2 and its combustibility make researchers reluctant to use this gaseous RA. Apparently, a great challenge being encountered in nanoscience fields is to exploit a straightforward, economically viable, and “green” approach to yield monodisperse metal and semiconductor nanoparticles at ambient temperature and within a short time. Herein, we present a novel and facile approach to rapidly synthesize and effectively stabilize relatively monodisperse Au nanocrystals by employing non-toxic renewable biochemical of β -D-glucose and by simply adjusting the pH value in the environmentally benign medium of H_2O , which fully adopts the fundamental principles^[9] of the “green” chemistry. Importantly, the Au nanocrystals thus prepared (protected by β -D-glucose) were found to function as effective catalyst to activate the reduction of 4-nitrophenol (to form 4-aminophenol) in the presence of NaBH_4 , otherwise unfeasible if only the strong reducing agent NaBH_4 is employed. Also, it is worth noting that there are several significant merits in the current synthesis strategy. First, the β -D-glucose can act both as RA and CA for the generation of Au nanocrystals upon the addition of basic aqueous solution; Second, the highly stable Au nanocrystals (at least persist six months in aqueous solution) could be achieved by simply adjusting the pH environment in the system. Additionally, one may separate CA of β -D-glucose from Au nanocrystals at relatively high temperature or by utilizing phase-transfer reactions,^[10] in consideration of weak hydrogen-bonding interactions between β -D-glucose and the surface of the nanocrystals. Finally, glucose is a biologically compatible “green” chemical, thus the glu-

cose-protected nanoparticles can be easily integrated into systems relevant for pharmaceutical, biomedical, and biosensor applications. Accordingly, the exploitation of such a system presents tremendous opportunities and advantages in the bottom-up development of the modern nanotechnological science and industry.

Results and Discussion

UV/Vis studies on Au nanoparticles: Although β -D-glucose is well known as a reducing sugar, it does have limited reduction ability at ambient temperature. However, β -D-glucose can effectively reduce Au^{3+} ions into Au^0 upon the addition of a small amount of NaOH aqueous solution; this was confirmed by both of visual observation and accurate UV/Vis determination. The system finally turned a red wine color after the reduction reaction, as shown in Figure 1

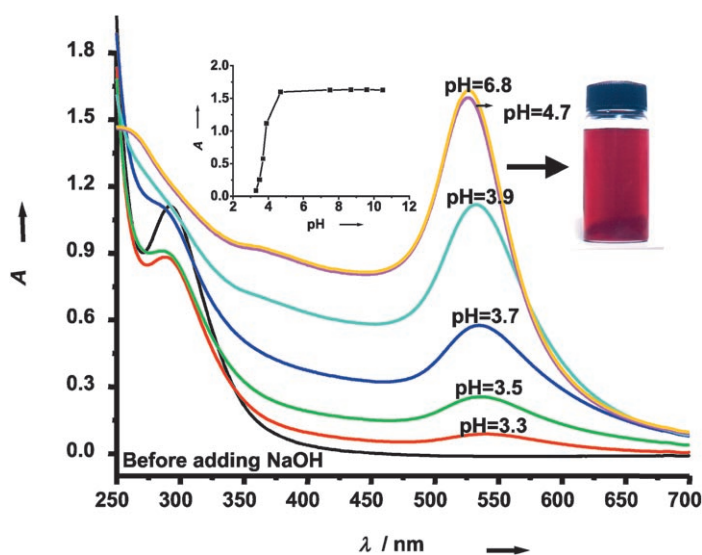
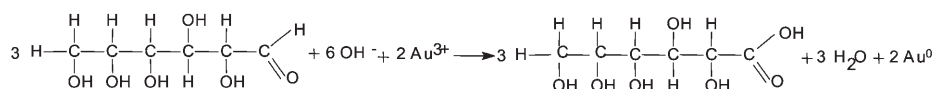
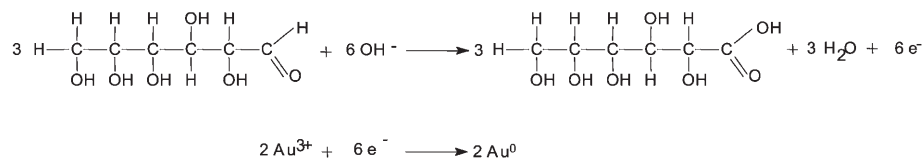


Figure 1. The UV/Vis absorption spectra of the Au nanoparticles stabilized in a 0.03 M aqueous β -D-glucose dispersion under different pH conditions (the insets present the reaction kinetic graph for the formation of Au nanoparticles as well as the digital image of aqueous Au-nanoparticle dispersions at a pH of 6.8).

(inset), visually manifesting the formation of Au nanoparticles. The UV/Vis absorption spectra exhibiting reaction evolution are also presented in Figure 1. As shown in Figure 1, the absorption peak of HAuCl_4 at about 290 nm decreases gradually and finally disappears (upon the continual addition of NaOH aqueous solution in the system); this disappearance is concomitant with the appearance of a new characteristic absorption band originating from the surface-plasmon resonance of nanometer-sized Au particles.^[11] The surface-plasmon absorption band undergoes a slight blue shift from 537 to 525 nm with the increase of pH value; this shift might be due to a decrease in the size of Au nanoparticles formed.^[12] Additionally, the intensity of Au nanoparticles absorption peak increases with increasing pH value until the

pH reaches a value of 6.8, after that the further increase of pH value has no significant effect on the Au-nanoparticle absorption intensity. To clearly exhibit the reaction dynamics of the formation of Au nanoparticles with the quantitative change of OH^- , the dependence of the Au-nanoparticle absorption intensity on the pH value of the system is also provided in Figure 1 (inset). The reduction reaction equation^[13] shown in Scheme 1 clearly indicates that the OH^- ion is involved in the reaction to yield Au nanoparticles, consistent with the visual observation and UV/Vis experimental results described above. It should be mentioned here that although β -D-glucose in the equation is presented as an open chain format, in reality, the majority of the structure of the β -D-glucose in aqueous solution is in the cyclic chair form. Accordingly, it is convincing that β -D-glucose not only serves the function of effective RA to reduce Au^{3+} to the ground state rapidly at ambient temperature (in the presence of OH^-), but also operates as CA to passivate the surface and prevent the growth of Au nanoparticles (this will



Scheme 1. The reduction reaction equation for the formation of Au nanoparticles.

be further discussed below) in the system; besides, the pH environment has an appreciable influence on the Au nanoparticle synthesis due to the involvement of OH^- in the reduction reaction.

The effect of β -D-glucose concentration on the UV/Vis absorption spectra of Au nanoparticles synthesized at a constant pH environment (7.0) is shown in Figure 2. In agreement with Mie's theory,^[12] the surface-plasmon maximum absorption wavelength of Au nanoparticles (λ_{max}) shifts to a lower value with decreasing the size of Au nanoparticles. Thus, it is easy to understand from Figure 2 that the size of Au nanoparticles decreases with the increase of β -D-glucose concentration, as evidenced by the occurrence of a blue shift of Au nanoparticles λ_{max} (from 568 to 517 nm) with the increase of β -D-glucose concentration within the concentration range studied (from 5×10^{-3} to 5×10^{-2} M). Thus it is easy to deduce that the higher the β -D-glucose concentration, the more effective the capping function of the β -D-glucose and the more nucleation sites the β -D-glucose provides to finally result in smaller Au nanoparticles. These results, on the other hand, further reveal the pivotal role of the β -D-glucose (acting as a CA) in the generation of nanoscale Au particles.

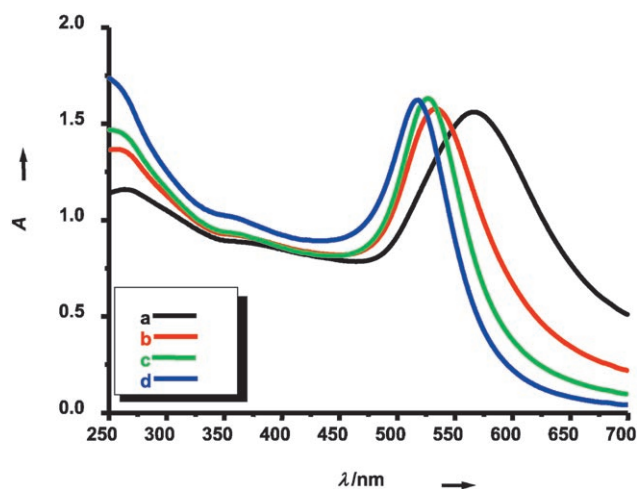


Figure 2. UV/Vis absorption spectra of the Au nanoparticles stabilized in different concentration β -D-glucose dispersions (a: 5×10^{-3} M; b: 1×10^{-2} M; c: 3×10^{-2} M; d: 5×10^{-2} M) at pH of 7.0.

Fourier transform IR (FT-IR)

characterization: The interaction between Au nanoparticles and β -D-glucose through an hydroxyl group was investigated by the comparison of FT-IR spectra of pure β -D-glucose and Au nanoparticles fabricated in aqueous β -D-glucose dispersions. Figure 3a shows the pure β -D-glucose IR spectrum in which a broad band at 3260 cm^{-1} is observed. Undoubtedly, this peak results

from the $-\text{OH}$ stretch of β -D-glucose molecules. Upon reduction, stabilization by β -D-glucose and subsequent elaborate separation of the Au nanoparticles (see Experimental Section), a strong absorption peak at 3395 cm^{-1} is observed (Figure 3b), manifesting the presence of β -D-glucose as an

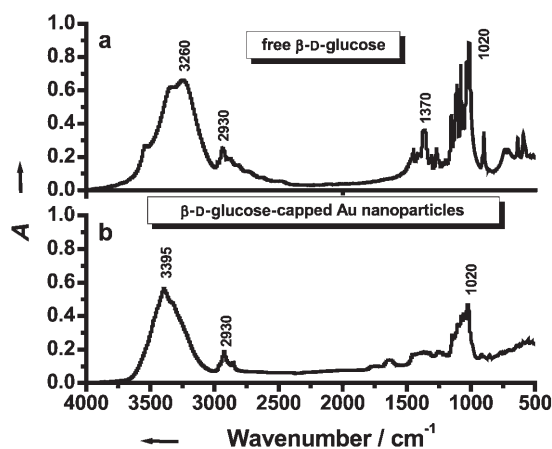


Figure 3. FT-IR spectra of a) free β -D-glucose and b) β -D-glucose-coated Au nanoparticles.

essential component of the Au nanoparticles. In addition, the absorption band of the -OH stretching mode undergoes a significant high-frequency shift—from 3260 to 3395 cm^{-1} —suggesting the intimate association (which will be discussed in detail in the mechanism section) between $\beta\text{-D-glucose}$ and the surface of the Au nanoparticles.

Morphologies of the Au nanoparticles: A typical TEM image of Au nanoparticles formed is displayed in Figure 4. As we anticipated from the absorption data and FT-IR evidence, the characteristic spherical Au nanoparticles are observed with a relatively narrow particle size distribution (5–13 nm range). In addition, a few triangular Au nanoparticles also appear in the image; similar morphologies for Au and Ag nanoparticles were observed previously.^[14] A histogram of Au particle size distribution is also presented in Figure 4

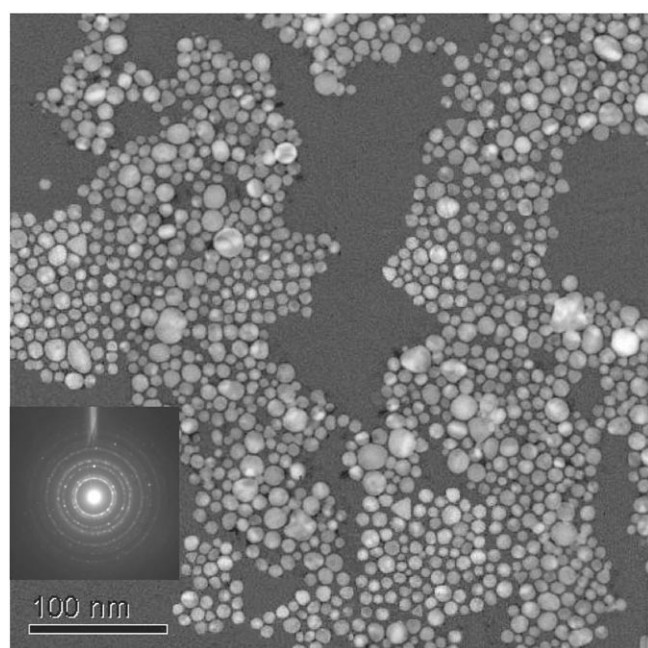


Figure 4. Representative TEM image of the Au nanoparticles stabilized by 0.03 M $\beta\text{-D-glucose}$ at a pH of 6.8 (Scale bar: 100 nm) together with a histogram of the Au nanoparticles size distribution. The inset is the ED pattern of the Au nanoparticles.

(the triangular Au nanoparticles are excluded from the statistics). The mean particle diameter observed is 8.2 nm (standard deviation, $\text{SD}=2.3\text{ nm}$) and more than 97% of the nanoparticles are in the size range from 5 to 11 nm, indicating a relatively high monodispersity of the Au nanoparticles formed in the system. To clarify the exact crystal structure of the Au nanoparticles, electron diffraction (ED) measurements were carried out. The diffraction rings of the Au nanoparticles ED pattern (inset in Figure 4) correspond well to the crystalline planes of the face-centered-cubic (fcc) structured Au,^[15] suggesting the crystalline nature of these Au nanoparticles.

Additionally, the multiple lattice fringes with an interplanar spacing of 2.33 \AA (consistent with the interplanar distance of (111) plane) can be observed clearly by using high-resolution TEM (Figure 5), further confirming the crystal-

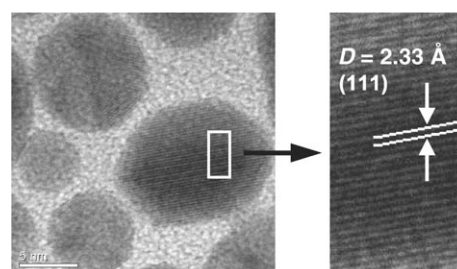


Figure 5. High-resolution TEM images of Au nanoparticles formed in the system (the scale bars equal 5 nm).

line nature of the Au nanoparticles formed. Furthermore, the X-ray diffraction (XRD) pattern of Au nanoparticles is presented in Figure 6, in which the diffraction peaks for the

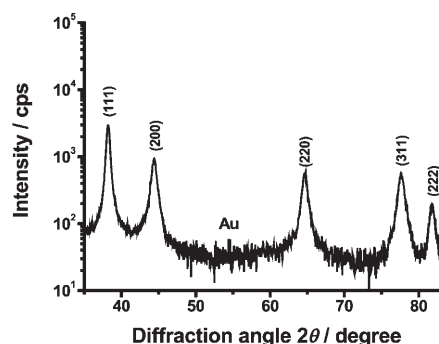


Figure 6. XRD pattern of Au nanocrystals formed in the system.

(111), (200), (220), (311), and (222) lattice planes appear clearly. Thus, the XRD results further corroborate the fcc structure nature of Au nanocrystals (consistent with the ED results) formed in the system. From the Scherrer equation^[16] together with the XRD data in Figure 6, the average Au particle size was estimated to be 8.9 nm ($\text{SD}=1.3\text{ nm}$) which is consistent with the TEM observation (8.2 nm, $\text{SD}=2.3\text{ nm}$).

The stability and separation of Au nanoparticles: The stability of nanoparticles is a key issue in consideration of the aggregation of nanoparticles after a long storage time in the reaction media. In the current system, it was surprisingly found that not only did the OH^- ions involve in the reaction for the formation of Au nanoparticles, but also the pH environment had a significant influence on the particle stability. Seven sets of Au nanoparticle stabilization experiments were performed at different pH values of 3.7, 4.0, 4.5, 6.5, 8.3, 9.7, and 10.2 in 0.03 M aqueous β -D-glucose dispersions. The Au nanoparticles were not so stable at low pH, in the range from 3.7 to 4.5, according to the simple visual observation of the solution color change and the appearance of large Au particle aggregates precipitated on the bottom of the bottle within two weeks. While at high pH, in the range from 6.5 to 10.2, the Au nanoparticle dispersions were stable for a prolonged duration (at least six months observation period) and did not show any color change and signs of aggregation and precipitation.

Interestingly, when the aqueous β -D-glucose-stabilized Au nanoparticle dispersions were highly centrifuged (with a speed of 6000 rpm), a significant amount of Au nanoparticles precipitated were observed on the bottom of the centrifuge tube consistent with weakening solution color; however, these particles were found to be completely soluble in aqueous solution again after shaking of the centrifuge tube. This indicates that the β -D-glucose-capped Au nanoparticles have a virtue of being repeatedly isolated from and redissolved in aqueous solutions without irreversible aggregation or decomposition.

Capping mechanism of β -D-glucose: The exact capping mechanism of β -D-glucoses on the formation of Au nanoparticles and the effect of pH environment on the stability of nanoparticle dispersions are interesting topics of the current investigation. The five hydroxyl groups in the β -D-glucose molecule can, in the present case, facilitate the complexation of Au nanoparticle to the molecular matrix of β -D-glucose. Previous reports on the measurement of ξ potential^[6,17] of Au nanoparticles as the function of pH value confirmed the presence of a pH-dependent equilibrium between $-\text{OH}$ and $-\text{O}^-$ on the Au surface. The equilibrium dynamics are dictated by the pH environment relative to the $\text{p}K$ value of the hydroxylated surface of particle. When the pH is below the $\text{p}K$ value, $-\text{OH}$ is dominant; otherwise, $-\text{O}^-$ is dominant. The oxidized portion of the particle surface should mainly have $\text{Au}-\text{O}^-$ groups at a high pH ($>\text{p}K$) and increasing numbers of $\text{Au}-\text{OH}$ groups at low pH ($<\text{p}K$).^[6,17] This may explain plausibly the role of β -D-glucose as a CA and the pH dependence on the stability of Au nanoparticles dispersion. A high pH value (around 6.8–10.5) favors the occurrence of $\text{Au}-\text{O}^-$ groups (on the Au nanoparticle surface) that can interact with hydroxyl groups of the β -D-glucose through hydrogen bonding, resulting in the effective coverage of the β -D-glucose on the surface of Au nanoparticles. While at low pH (around 3.7–4.5), the abundance of the $\text{Au}-\text{OH}$ groups leads to a only to a weak hydrogen bonding

interaction between the β -D-glucose and the surface of Au nanoparticles that is not strong enough to stabilize the particles for a long duration.^[6,17] Recent results from our group show that the β -D-glucose-stabilized Au nanoparticles could be self-assembled into nanowires and mesoporous network at high basic aqueous solution ($\text{pH} > 11.5$),^[18] suggesting the vital association of pH environment with the self-assembly of β -D-glucose-stabilized Au nanoparticles.

Catalytic function of Au nanoparticles: One of the important applications of the metal nanoparticles is to activate/catalyze some reactions that are otherwise unfeasible. To this end, the catalytic function of β -D-glucose-capped Au nanoparticles on the reduction of 4-nitrophenol was investigated in the study. It is seen that an absorption peak of 4-nitrophenol undergoes a red shift from 317 to 400 nm (due to the generation of 4-nitrophenolate ion) immediately upon the addition of aqueous solution of NaBH_4 (15 mM), corresponding to a significant change in solution color from light yellow to yellow-green (inset of Figure 7, right-hand image).

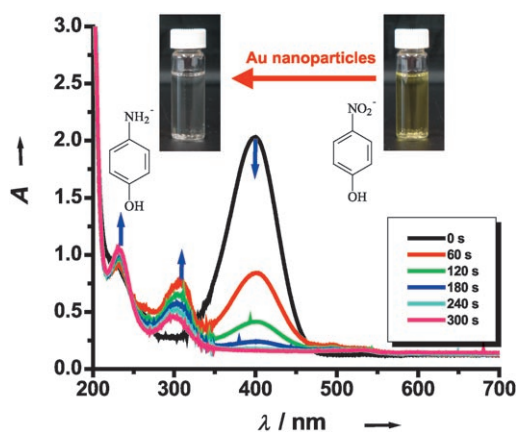


Figure 7. Successive UV/Vis absorption spectra of the reduction of 0.20 mM 4-nitrophenol by 15 mM NaBH_4 in the presence of β -D-glucose-capped Au nanoparticles (0.2 mM) as catalyst.

In the absence of catalyst of Au nanoparticles, the absorption peak at 400 nm remained unaltered for a long duration, indicating the inability of the strong reducing agent NaBH_4 itself to reduce 4-nitrophenolate ion. Interestingly, the addition of an aliquot of Au nanoparticles (0.2 mM) dispersion to the reaction system caused a fading and ultimate bleaching of the yellow-green color of 4-nitrophenolate ion in aqueous solution (inset of Figure 7), suggesting the occurrence of the reduction reaction. The UV/Vis spectra in Figure 7 unambiguously verify this conclusion as well, as the absorption band of 4-nitrophenolate ion at 400 nm decreases and disappears within five minutes of the addition of Au nanoparticles, with the concomitant appearance of two new peaks at 300 nm and 230 nm, respectively (attributed to the generation of 4-aminophenol). To exclude the possibility that the reduction reaction might be activated by the reducing sugar of β -D-glucose instead of Au nanoparticles, an aliquot of an

aqueous β -D-glucose dispersion (0.03 M) alone was added into 4-nitrophenol (0.20 mM) and NaBH_4 (15 mM) mixture aqueous solution. No change in the color and position of the absorption band (at 400 nm) of 4-nitrophenolate ion was observed. Thus, the reduction of 4-nitrophenol by NaBH_4 has been clearly demonstrated to be activated by β -D-glucose-capped Au nanoparticles. Since the concentration of BH_4^- added in the system is much higher in comparison with that of 4-nitrophenol, it is reasonable to assume that the concentration of BH_4^- remains constant during the reaction. In this context, pseudo-first-order kinetics could be used to evaluate the kinetic reaction rate of the current catalytic reaction, together with the UV/Vis absorption data in Figure 7. As expected, a good linear correlation of $\ln(A)$ versus time (A is the absorption intensity of 4-nitrophenolate ion) obtained (Figure 8), whereby a kinetic reaction rate constant is esti-

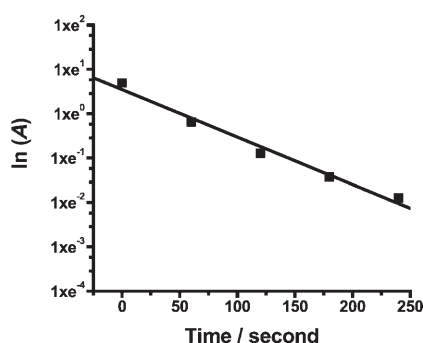


Figure 8. Plot of $\ln(A)$ against time for the Au nanoparticles catalytic reduction of 4-nitrophenol.

mated to be $6.54 \times 10^{-3} \text{ s}^{-1}$. This value is comparable to that of other nanoparticle catalysts for the reduction of the 4-nitrophenol in the presence of NaBH_4 .^[19] The catalysis of the Au nanoparticles is possibly due to the efficient electron transfer from BH_4^- ion to nitro compounds mediated by the nanoparticles. This could be attributed to the higher driving force of particle-mediated electron transfer caused by their large Fermi level shift^[20] in presence of highly electron-injecting species such as borohydride ions.

Conclusion

In summary, a facile, economically viable and “green” approach for the synthesis of relatively monodisperse Au nanocrystals (average diameter = 8.2 nm, SD = 2.3 nm) has been developed by employing β -D-glucose both as RA and the CA under controlled pH environments. The Au nanocrystals could be synthesized rapidly at ambient conditions in the system. Also, the catalytic function of the Au nanoparticles to activate the reduction of 4-nitrophenol in the presence of NaBH_4 has been clearly confirmed by both visual observation and UV/Vis spectra. This Au-nanoparticle synthesis approach could be reasonably extended to the preparation of other metal nanoparticles and is currently

under the further investigation. Also, it is very important to explore the pharmaceutical, biomedical, and biosensor applications of the β -D-glucose-coated metal nanoparticles by virtue of the biologically compatible characteristic of the β -D-glucose.

Experimental Section

Materials: $\text{HAuCl}_4 \cdot 3\text{H}_2\text{O}$ as the precursor for the formation of Au nanocrystals was purchased from Acros Organics. β -D-Glucose acting both as reducing agent and capping agent was supplied from Sigma. Deionized water obtained from Fisher Scientific was used in all experiments. Sodium hydroxide (NaOH), sodium borohydride (NaBH_4), and 4-nitrophenol were products from Acros Organics.

Preparation of nanoparticles: The Au nanoparticles were synthesized by the reduction of Au^{3+} ions in the aqueous β -D-glucose dispersions. The approach was quite straightforward. In a typical preparation, an aqueous solution of $\text{HAuCl}_4 \cdot 3\text{H}_2\text{O}$ (0.05 M; 200 μL aliquot) was added to an aqueous solution of β -D-glucose (0.03 M; 50 mL). The solution was stirred for more than 30 minutes and no color change was observed, indicating that the reduction reaction did not occur in the system. Subsequently, an aqueous solution of NaOH (0.05 M) was continuously added dropwise to the system until there was no further change in solution color. During the addition of NaOH , the reaction dynamics for the formation of Au nanoparticles was systematically investigated at a pH range from 3.3 to 10.5 by using a Jasco V-570 UV/Vis spectrophotometer. The pH values of the Au colloid solution were accurately measured by a TOA pH meter (HM-30 s) with a Combination Electrode (GST-5311C, TOA Electronics Ltd) upon 30 mins after the initial formation of the solution.

Preparation of FT-IR samples: The aqueous Au-nanoparticle dispersion was first centrifuged for about 20 minutes with speed of 6000 rpm, whereby a significant amount of Au nanoparticle were deposited on the bottom of the centrifuge tube. The precipitated Au nanoparticles were then carefully isolated by using a polyethylene transfer pipette inserted into the bottom of the centrifuge tube. The performance was repeated three times to give a highly concentrated Au-nanoparticle dispersion; most of unbonded β -D-glucose and isolated ions remained in the upper aqueous phase in the centrifuge tube. A centrifugal membrane with a molecular weight cutoff of 3000 (PALL Life Science) was subsequently employed to further remove excess β -D-glucose and isolated ions. Afterwards, freeze drying under vacuum was applied overnight to get the very dry composite Au nanoparticles. Finally, the FT-IR samples were obtained by forming thin transparent KBr (95 mg) and Au nanoparticles (1 mg) pellet. A pure 100 mg KBr pellet used as background was subtracted from the FT-IR spectra of the Au nanoparticle sample. All the FT-IR spectra were recorded on a Nicolet AVATAR 360 ESP spectrometer (Nicolet, Madison, WI, USA).

Catalytic reduction of 4-nitrophenol: The catalytic reduction reaction was occurred in a standard quartz cell with a 1 cm path length and about 3 mL volume. The reaction procedures were as follows: NaBH_4 (1 mL of a 15 mM solution in water) was mixed together with 4-nitrophenol (1.7 mL of a 0.20 mM solution in water) in the quartz cell; this lead to the change of color from light yellow to yellow-green. Immediately after addition of Au nanoparticles (0.3 mL of a 0.2 mM of an aqueous dispersion), the absorption spectra were recorded by a Jasco V-570 UV/Vis spectrophotometer with a time interval of 60 seconds in a scanning range of 200–700 nm at room temperature of 25 °C.

Morphology and crystallinity studies: The sample grids for TEM measurements were prepared by placing a drop of aqueous Au nanoparticles dispersion onto the copper grids and subsequently evaporating water naturally overnight at ambient condition. The morphology and size distribution of the Au particles were determined by a Hitachi H-800 TEM at an operating voltage of 200 kV. The crystallinity of the Au nanoparticles was studied by XRD (Rigaku RINT 2200 diffractometer) with $\text{Cu}_{K\alpha}$ radiation (40 kV and 20 mA) and ED techniques.

Acknowledgements

The authors also gratefully acknowledge financial support from the Japan Society for the Promotion of Science (JSPS) and the CREST program of Japan Science and Technology Agency (JST).

- [1] a) A. I. Cooper, *Adv. Mater.* **2001**, *13*, 1111; b) J. D. Holmes, D. M. Lyons, K. J. Ziegler, *Chem. Eur. J.* **2003**, *9*, 2144; c) K. P. Johnston, P. S. Shah, *Science* **2004**, *303*, 482; d) J. L. Zhang, B. X. Han, J. C. Liu, X. G. Zhang, Z. M. Liu, J. He, *Chem. Commun.* **2001**, 2724; e) J. L. Zhang, B. X. Han, J. C. Liu, X. G. Zhang, J. He, Z. M. Liu, *Chem. Eur. J.* **2002**, *8*, 3879; f) K. J. Ziegler, R. C. Doty, K. P. Johnston, B. A. Korgel, *J. Am. Chem. Soc.* **2001**, *123*, 7797; g) P. Raveendran, J. Fu, S. L. Wallen, *J. Am. Chem. Soc.* **2003**, *125*, 13940; h) J. C. Liu, P. Raveendran, Z. Shervani, Y. Ikushima, *Chem. Commun.* **2004**, 2582.
- [2] a) M. Brust, M. Walker, D. Bethell, D. J. Schiffrin, R. Whyman, *J. Chem. Soc. Chem. Commun.* **1994**, *7*, 801; b) A. Ullman, *Chem. Rev.* **1996**, *96*, 1533; c) S. H. Sun, C. B. Murray, D. Weller, L. Folks, A. Moser, *Science* **2000**, *287*, 1989; d) N. Q. Wu, L. Fu, M. Su, M. Aslam, K. C. Wong, V. P. Dravid, *Nano Lett.* **2004**, *4*, 383.
- [3] a) P. S. Shah, J. D. Holmes, R. C. Doty, K. P. Johnston, B. A. Korgel, *J. Am. Chem. Soc.* **2000**, *122*, 4245; b) S. Y. Zhao, Z. H. Chen, D. G. Li, X. G. Yang, H. Y. Ma, *Phys. E* **2004**, *23*, 92.
- [4] a) C. Petit, P. Lixon, M. P. Pileni, *J. Phys. Chem.* **1993**, *97*, 12974; b) J. P. Cason, M. E. Miller, J. B. Thompson, C. B. Roberts, *J. Phys. Chem. B* **2001**, *105*, 2297.
- [5] a) M. C. McLeod, R. S. McHenry, E. J. Beckman, C. B. Roberts, *J. Phys. Chem. B* **2003**, *107*, 2693; b) J. C. Liu, P. Raveendran, Z. Shervani, Y. Ikushima, Y. Hakuta, *Chem. Eur. J.* **2005**, *11*, 1854; c) K. Kim, D. Demberelnyamba, H. Lee, *Langmuir* **2004**, *20*, 556.
- [6] J. Sylvestre, A. V. Kabashin, E. Sacher, M. Meunier, J. H. T. Luong, *J. Am. Chem. Soc.* **2004**, *126*, 7176.
- [7] a) Q. Y. Lu, F. Gao, S. Komarneni, *Adv. Mater.* **2004**, *16*, 1629; b) Q. Y. Lu, F. Gao, S. Komarneni, *Langmuir* **2005**, *21*, 6002; c) Z. H. Wang, J. W. Liu, X. Y. Chen, J. X. Wang, Y. T. Qian, *Chem. Eur. J.* **2005**, *11*, 160.
- [8] J. C. Liu, P. Raveendran, G. W. Qin, Y. Ikushima, *Chem. Commun.* **2005**, 2972.
- [9] P. T. Anastas, J. C. Warner, *Green Chemistry: Theory and Practice*, Oxford University Press, New York, **1998**.
- [10] a) J. C. Garcia-Martinez, R. W. J. Scott, R. M. Crooks, *J. Am. Chem. Soc.* **2003**, *125*, 11190; b) G. T. Wei, Z. Yang, C. Y. Lee, H. Y. Yang, C. R. C. Wang, *J. Am. Chem. Soc.* **2004**, *126*, 5036.
- [11] S. Link, M. A. El-Sayed, *J. Phys. Chem. B* **1999**, *103*, 4212.
- [12] G. Mie, *Ann. Phys.* **1908**, *25*, 377.
- [13] Fehling's tests (http://www.uni-regensburg.de/Fakultaeten/natFak_IV/OrganischeChemie/Didaktik/keusch/D-Fehling-e.htm) for aldehydes, which are similar with the β -D glucose reduction of the Au^{3+} (to form Au^0) in the presence of the OH^- are used extensively in carbohydrate chemistry.
- [14] a) S. Komarneni, H. Katsuki, *Pure Appl. Chem.* **2002**, *74*, 1537; b) S. Komarneni, D. Li, B. Newalkar, H. Katsuki and A. S. Bhalla, *Langmuir* **2002**, *18*, 5959.
- [15] M. Brust, J. Fink, D. Bethell, J. D. Schiffrin, C. Kiely, *J. Chem. Soc. Chem. Commun.* **1995**, 1655.
- [16] E. W. Nuffield, *X-ray diffraction methods*, Wiley, New York, **1966**
- [17] J. Sylvestre, S. Poulin, A. V. Kabashin, E. Sacher, M. Meunier, J. H. T. Luong, *J. Phys. Chem. B* **2004**, *108*, 16864.
- [18] G. W. Qin, P. Raveendran, J. C. Liu, T. Balaji, K. Oikawa, H. Matsunaga, H. Hakuda, K. Ishida, Y. Ikushima, unpublished results.
- [19] a) K. Hayakawa, T. Yoshimura, K. Esumi, *Langmuir* **2003**, *19*, 5517; b) K. Esumi, R. Isono, T. Yoshimura, *Langmuir* **2004**, *20*, 237.
- [20] a) I. Mora-Sero, J. Bisquert, *Nano Lett.* **2003**, *3*, 945; b) M. Jakob, H. Levanon, P. V. Kamat, *Nano Lett.* **2003**, *3*, 353.

Received: August 1, 2005

Published online: December 16, 2005